AUBE '01

12TH INTERNATIONAL CONFERENCE ON AUTOMATIC FIRE DETECTION

March 25 - 28, 2001
National Institute Of Standards and Technology
Gaithersburg, Maryland U.S.A.

PROCEEDINGS

Editors: Kellie Beall, William Grosshandler and Heinz Luck

NIST
National Institute of Standards and Technology
Technology Administration, U.S. Department of Commerce

Woo C. Kim, Yudaya R. Sivathanu, and Jay P. Gore
Mid Infrared Sensing Diagnostics and Control Consortium
School of Mechanical Engineering
Purdue University, West Lafayette, IN 47907-1003

Characterization of Spectral Radiation Intensities from Standard Test Fires for Fire Detection

Abstract

Spectral radiation intensities at 160 mid infrared wavelengths leaving six standard test fires specified in the guidelines of the European Committee for Standardization (ECN Fires) were measured. A recently developed Fast Infrared Array Spectrometer (FIAS) was utilized to acquire spectral radiation intensities in the 1.8 – 4.9 μm wavelength range from the transient as well as the steady burning fires. The mean and root mean square, the Probability Density Function (PDF), the Cumulative Probability Density Function (CPDF), and the Power Spectral Density (PSD) of the spectral radiation intensities were studied to characterize the fires. The spectral radiation intensity in the 4.3 μm micron carbon dioxide band is larger than that at other wavelengths for the open fires. The continuum radiation from soot particles dominates gas band radiation for the smoldering fires. The statistical characteristics of the fires depend on the fuel type, time after ignition and measurement wavelength and can be used in fire detection algorithms.

1. Introduction

Current residential fire detectors include optical smoke sensors, ionization smoke sensors, and temperature (heat) detectors [1]. These detectors have response times of the order of 2 to 20 minutes depending on the location of the fire relative to the detector because combustion products must travel to the detector location for the operation.

More recently, there has been increased interest in the use of radiation emission sensors (flame detectors) for faster fire detection compared to smoke and heat sensors [2]. A

combination of detectors may be necessary to detect fires that do not have significant radiation signatures. Single or multiple radiation-based fire detectors with ultraviolet, near infrared and mid infrared filters have been used under various conditions to allow detection with minimal false alarms. Ultraviolet signals are emitted by indoor radiation sources such as incandescent lights, arc welding processes, etc. Therefore, ultraviolet sensors are limited to outdoor usage where interfering solar radiation is absorbed by the earth's atmosphere. Another disadvantage of ultraviolet flame detectors is that any contamination of the optical windows causes a significant loss of sensitivity. Sivathanu and Tseng [3] showed that a two-wavelength near infrared fire detector is capable of detecting fires from a wide variety of materials with low false alarm rates and fast response time. However, the near infrared fire detector can barely detect an indirect smoldering fire since the signals from these fires are very low in the near infrared. In addition, non-luminous fires [4], such as those burning alcohol were not detected.

Radiation emitted by a fire has two primary components: continuum radiation from glowing soot particles in the flame and various emission bands such as at 2.7 μm and 4.3 μm originating from carbon dioxide molecules and at 2.7 and 6.3 μm originating from the water vapor in the combustion products. The characteristic temperatures of most accidental fires are such that the continuum radiation peaks in the mid infrared region of the spectrum. These unique characteristics may allow development of multi-wavelength fire detectors that recognize the spectral characteristics to avoid false alarms.

Past studies of spectral radiation properties of flames have involved luminous and non-luminous laboratory flames. These have included turbulent jet diffusion flames and pool fires. Two-wavelength pyrometric measurements conducted by Sivathanu and Faeth [5], Sivathanu et. al. [6], and Sivathanu and Gore [7] in luminous pool and jet fires indicate that the peak temperatures within these fires are in the range 1400 ± 300 K. Other radiation properties of the fires include the Probability Density Functions (PDFs) and the Power Spectral Densities (PSDs) of the turbulent fluctuations.

These characteristics can be used to design fire detectors that can avoid false alarms. However, other than the pool fires, which can occur in fire accidents, the fire spectral

radiation intensities have not been studied in the literature. Based on the background information provided above, measurements of the spectral radiation intensities in the mid infrared part of the spectrum leaving standard test fires conforming to the European Committee for Standardization - CEN-54 (ECN) [8] were measured. These data can contribute to advanced fire detection algorithm.

2. Experimental apparatus and method

To obtain measurements of spectral radiation intensities from fires for fast and reliable fire detection, the use of fast spectrometer is required, because the instantaneous intensities at different wavelengths should be used to analyze the frequency contents of six standard ECN fires. In particular, emissions of radiation from soot fluctuate at a higher frequency and have larger fluctuation intensity than the emission of gas band radiation. Hence, measurements were made using Fast Infrared Array Spectrometer (FIAS) to acquire spectral radiation intensities at 160 pixels in the 1.8 – 4.9 μm wavelength ranges and this unit is able to capture instantaneous spectra from the fires at a rate of 390 Hz. Findings by Ji, et al. [9] show that the agreement between the FIAS measurements and the previous data is very good.

FIAS was aimed at different angles and positions depending on whether the test fire is developing with time or not, assuming that all test fires are axisymmetric. For the transient test fire, – open cellulosic fire (TF1), smoldering pyrolysis fire (TF2), glowing smoldering fire (TF3), and open plastics fire (TF4) - the FIAS view angle is set at 45 degrees from the gravitational direction, where the angle is defined as shown in Figure 1., and a different radius from the flame axis, and time dependent data are acquired in a fixed position. For the TF1, TF2, and TF3, the FIAS is located at 300 mm in radial direction and 500 mm for TF4.

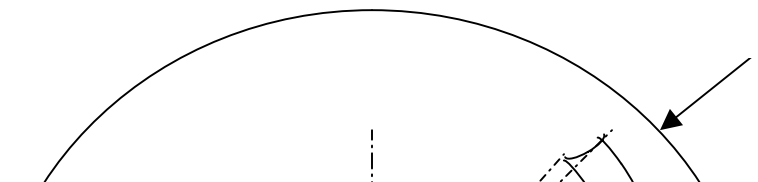

Figure 1. Schematic of defining the direction viewed by the FIAS
for the TF1, TF2, TF3, and TF4

The present work involves utilization of fire radiation for detection and generally the need for early fire detection suggests that the fire is smaller than the size of the enclosure at the time of detection. Therefore, in the case of the steady state test fires – liquid fire (n-heptane, TF5), and liquid fire (ethanol, TF2) -, intensities leaving the fire at four different heights were collected as representative values of fire development, and schematic diagram for experimental facility is shown in Figure 2.

Detailed descriptions of ECN fires are provided in Ref. [8]. The dimensions of TF1 were scaled down to one half so as to be able to accommodate our laboratories. The liquid fires stabilized on a water-cooled 15 cm diameter stainless steel burner. The height of the burner is 10 cm and the flame was stabilized with a lip height (depth of liquid surface below the pool edge) of 10 mm. The pool fires reached a steady state operating condition in approximately 3 to 4 minutes.

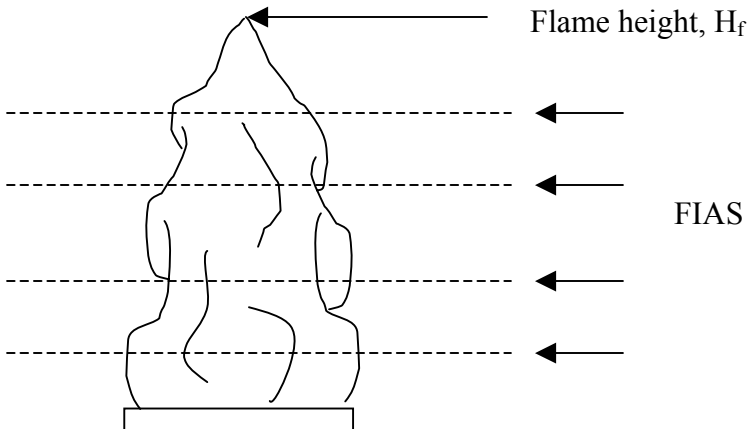

Figure 2. Schematic of defining the direction viewed by the FIAS for TF5 and TF6

3. Results and Discussion

3.1. General descriptions about standard test fires

The TF1 lasted around 13 minutes before going out automatically. During the first 5 minutes, the infrared signature from the methylated spirit dominated the spectral radiation intensities from the wooden crib, however in 5 minutes, the instantaneous spectral radiation intensities from both gas band and in-flame soot resulting from the fire grew and reached peak values around 9 minutes after ignition.

The TF2 began smoldering in 5mins and flame was made automatically in 9mins. Because the FIAS was aimed at the beechwood sticks, the infrared signatures from the TF2 were low compared with other standard test fires.

For the TF3, the igniter flames were immediately put out after ignition, and the cotton wicks continued to glow for the duration of the test.

The TF4 lasted around 7 mins and reached its peak intensities in 4mins.

TF5 is luminous and emit radiation from both soot and combustion products. The radiation heat flux directly contributes to the hazard posed by the flame and the spread rate of the fire. Fuels of similar composition, such as fuels classified as paraffin or alcohols generally have comparable flame shapes. The alcohol fuels, TF6, generally

necked in just above the burner lip and the paraffin (n-heptane) fuels had a larger distance before necking begins.

3.2. Mean Values of Spectral Radiation Intensities during 12.8sec

Figure 3 represents the mean spectral radiation intensities during 12.8 sec for all six standard test fires. Care should be taken for the scales of ordinate, because the radiation signature from TF2 was too small to keep the same scale with the other fires. One more thing to keep in mind is that the positions of FIAS are different between the transient TFs and steady state ones as we discussed earlier.

The TF1 and TF4 are very luminous and both gas band radiation and continuous soot radiation are evident. The radiation intensity from carbon dioxide and soot at 4.3 μm is more than two orders higher than that from soot, water, and carbon dioxide at 2.7 μm, which is similar to the spectral distributions observed in the open pool fires (TF5 and TF6).

For the two smoldering fires, TF2 and TF3, the continuous radiation from the smoldering surface is evident and the gas band radiation is hardly found, furthermore, the absorption in the carbon dioxide band in the room air at 4.3 μm is seen. Using Wien's displacement law to estimate temperature of the TF3, the temperature of inflame soot is 1024 K.

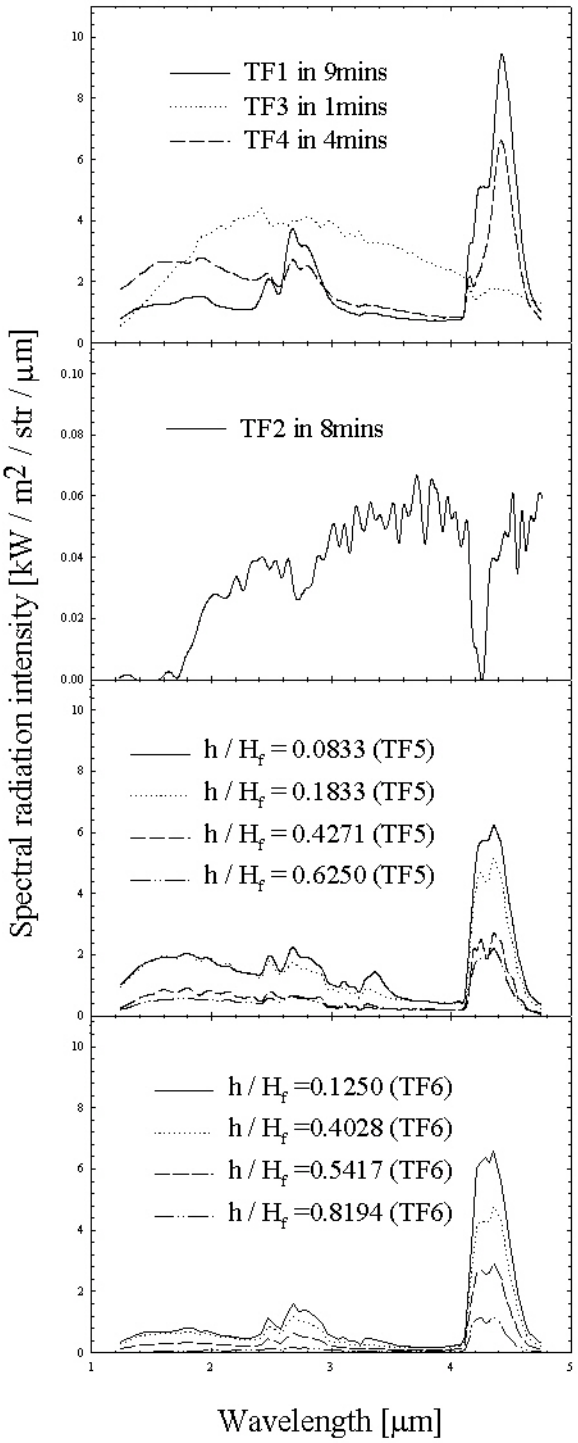

Figure 3. Spectral radiation intensities in TFs during 12.8 sec

The flame height of the TF5 and TF6 is 480 mm, 360 mm respectively, measured by visual inspection and four different dimensionless flame heights from the lip of the

flame are shown. Radiation from the CO_2 band and the H_2O band are evident in the spectra. However, the TF6 contains less soot than the TF5, and hence the radiation spectra are less dominated by soot. Radiation from H_2O becomes less intense as the dimensionless flame height increase. The continuum radiation for soot particles is also evident. As the dimensionless height increases, the spectral radiation intensities decrease. If we use Wien's displacement law to estimate the flame temperature associated with the maximum intensity of the soot radiation, a temperature of approximately 1630 K for the TF5 and 1476 K for the TF6 respectively, is obtained.

3.3. PDFs and CPDFs of spectral radiation intensities

The time series of normalized measured radiation intensities from inflame soot and the gas band at 1.45 μm, 2.47 μm, 2.68 μm, and 4.35 μm obtained from the test fires were analyzed to evaluate their Probability Density Function (PDF). The four wavelengths are selected to study the effects of soot radiation separately from those of soot+CO_2+H_2O radiation and soot+CO_2 radiation, and, to study the differences between the open fire, and smoldering fire, the PDFs of TF5 at $h/H_f = 0.0833$ and TF3 were chosen and shown in Figure 4.

Figure 4 illustrates that the PDFs are clipped Gaussian in shape, especially for the carbon dioxide and soot band at 4.3 μm, where carbon dioxide radiation is dominant, is almost symmetric around the mean intensity value, however the PDF at 1.45 μm for TF5, where in-flame soot dominates the spectral radiation intensity, is not symmetric in shape, and shows a lognormal behavior. Because of the large fluctuations in soot radiation, the overall ranges are broad.

Comparing the PDFs in TF3 with TF5, we can conclude that the PDFs are still Gaussian in shape, although there is some noise. However the TF3 continued to glow for the duration of the test and the fluctuation in radiation is not so high compared with TF6, the range of spectral radiation intensities is not so broad.

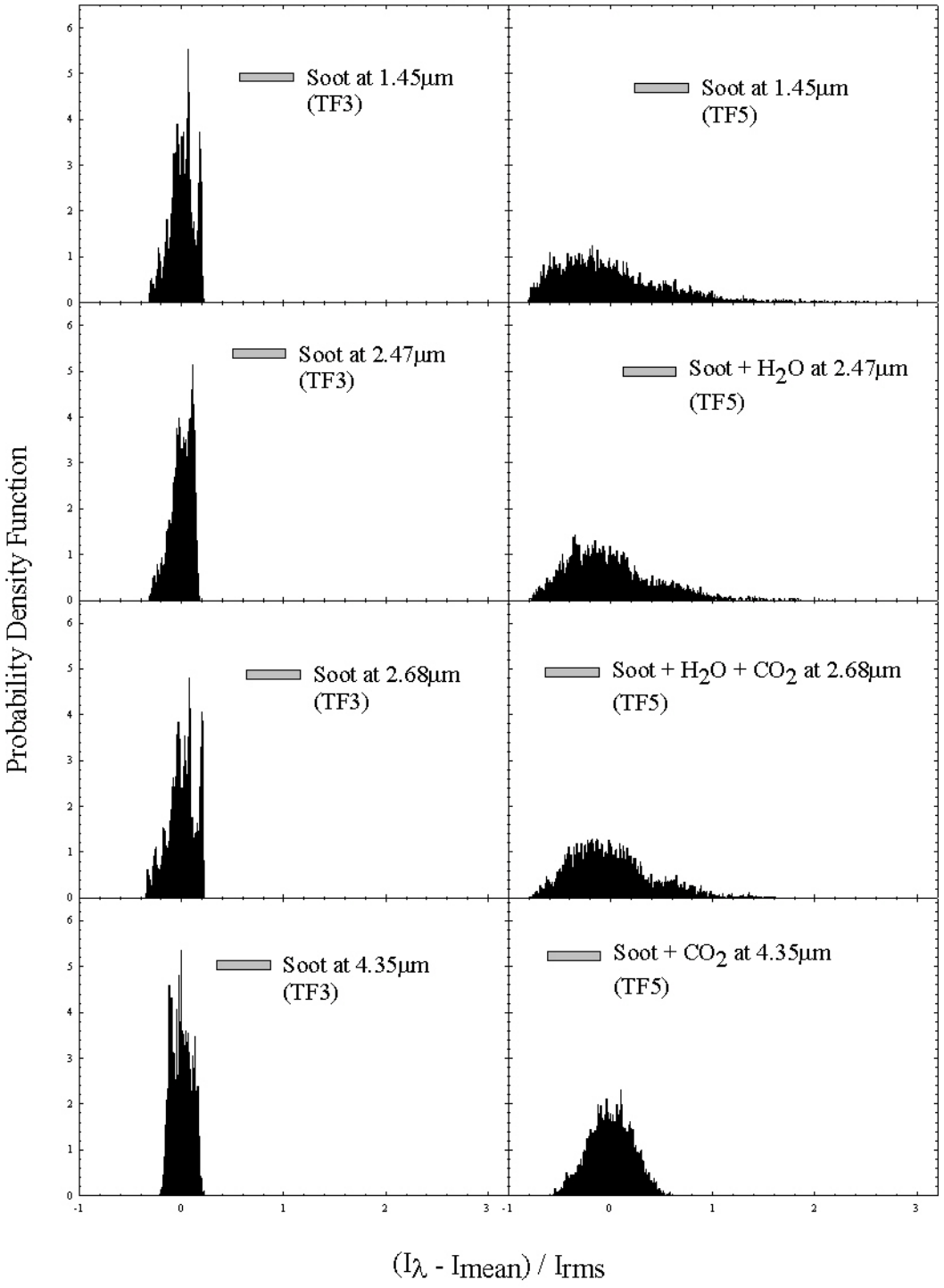

Figure 4. PDFs of spectral radiation intensities of TF3 and TF5 at $h/H_f = 0.0833$

The differences in the statistical behavior of intensities at different wavelengths can be examined in even greater detail by studying the Cumulative Probability Density

Function (CPDF) shown in Figure. 5, which shows CPDFs of TF3 and TF6 at h/Hf = 0.1250. The CPDF is an integral of the PDF and therefore less noisy. The information it presents consists of the intensity values at which the probability of occurrence of intensities below that value builds rapidly.

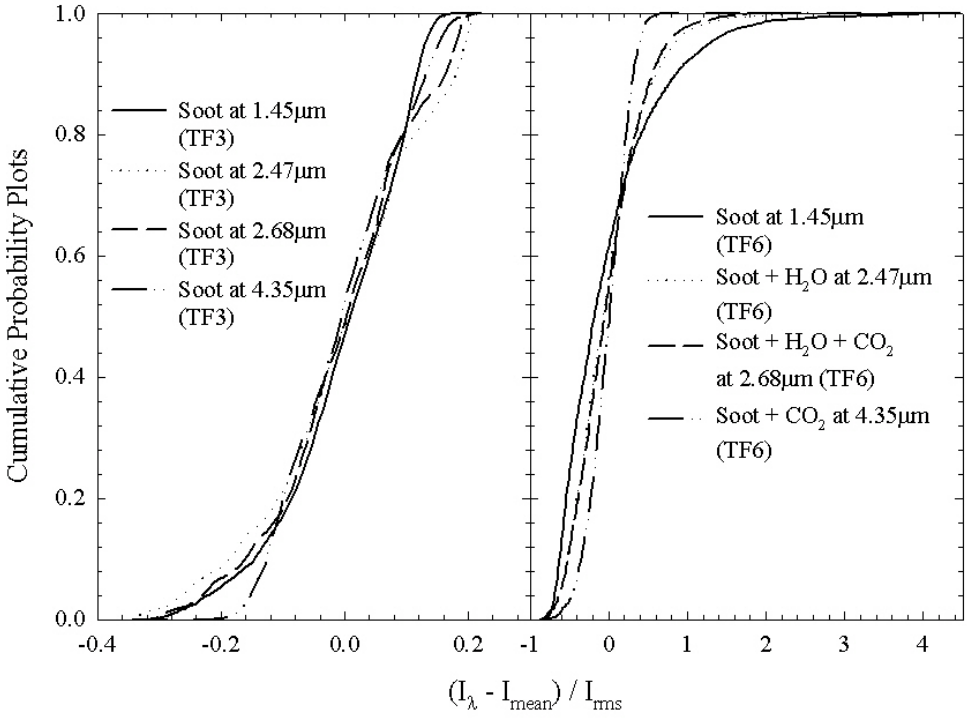

Figure 5. CPDFs of spectral radiation intensities of TF3 and TF6 at h/Hf = 0.1250

Figure 5 shows that the CPDF for intensities originating from the gaseous molecules rise very rapidly near a well-defined most probable value. In addition, the rise is the sharpest for the CO_2 band at 4.35 μm. The gas band CPDFs are steep because of the concentration fluctuations are strongly related to the level of mixing through the state relationships. The soot CPDF is flatter because various amounts of soot can exist at different levels of mixing depending on chemical kinetic and differential diffusion effects. Independent of the reasons for this, the characteristic that a flatter CPDF exists at soot wavelengths and a steeper CPDF exists at the gas band wavelengths can be used as an effective discrimination method in the sensor logic.

All the CPDFs of TF3 exhibit similar trend in slope because of the continuum emission from the same surface.

For the case of TF6, the PDFs of the soot+CO_2 and H_2O intensities at 2.47 μm and 2.68 μm respectively show a smaller weight in intensity near zero compared to the PDF of soot+CO_2 at 4.35 μm. This may be related to the self-absorption by cold CO_2 in the outer reaches of the flame at many instances. In addition, the soot+ CO_2 emission at 4.35 μm shows a clip at the highest intensity values. These results suggest caution regarding the use of this wavelength for fire detection. In addition, the result is also of relevance to the fundamentals of participating media heat transfer in fire and combustion environments.

3.4. PSDs of spectral radiation intensities

The Power Spectral Densities (PSDs) of spectral radiation intensities from the soot, CO2 and H_2O bands for TF3 and TF4 were analyzed to obtain their frequency content as shown in Figure 6. The PSD at the respective wavelengths were normalized by the mean-square fluctuations to compare with one another; hence the total area under each PSD is unity. The PSD is characterized by the flicker frequency and is determined by the size of the fire, the gravitational constant, and the turbulent flow established within the fire. The area under the PSD curve for any frequency range is proportional to the energy of the instantaneous fluctuations of the apparent source temperatures from the mean value. Although there is some noise around the Nyquist frequency of 195 Hz, this could be ignored considering the SN ratio.

It is important to note that the integrated infrared intensities do not show characteristic pulsation frequencies observed in planar imaging studies. There are commercial detectors that rely on pulsation frequencies and the present results do not support their sensor logic.

For the case of open fire, TF4, the PSD at the wavelengths (all wavelengths other than the 4.35 μm) dominated by soot radiation show higher energy content at higher frequencies compared to those dominated by the gas radiation (4.35 μm). This

characteristic of the sooty fires can also be utilized as a discriminator in fire sensor logic. Most of the energy of the fluctuations of the spectral radiation intensities is below 10-20 Hz and shows a decline to noise levels that are approximately five to six orders of magnitude lower for frequencies higher than 20 Hz.

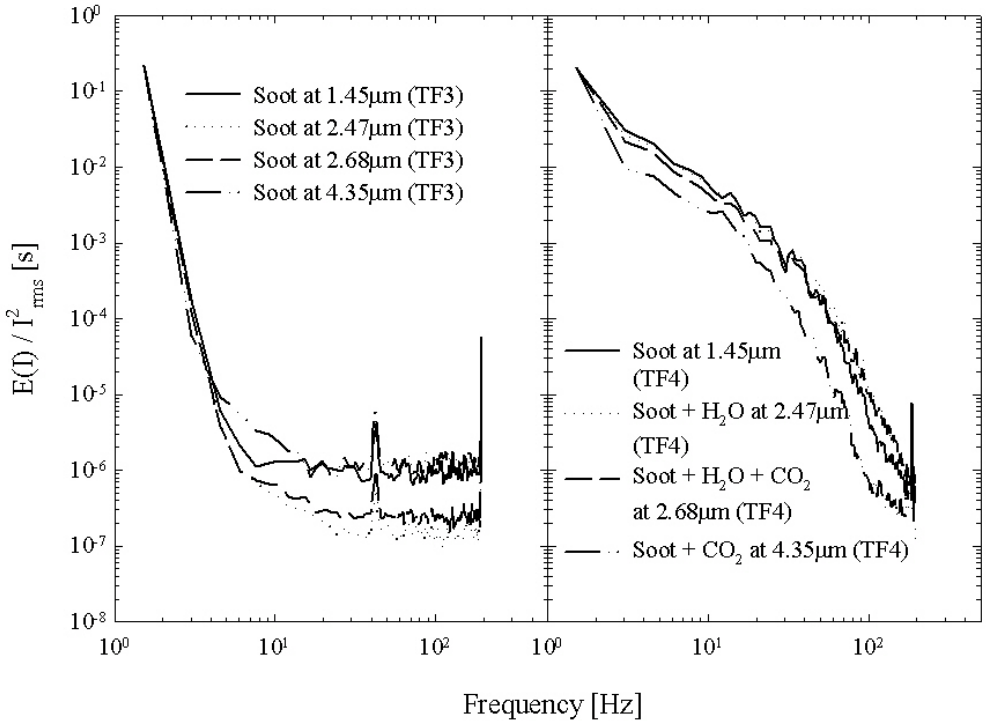

Figure 6. PSDs of spectral radiation intensities of TF3 and TF4

An interesting and most distinguishable feature of smoldering fire could be deduced from the left panel of Figure 6. Most of the energy of the fluctuations of the spectral radiation intensities is below 2 or 3 Hz and declines very rapidly to the noise levels that are approximately five to six orders of magnitude lower after 3 Hz. However, flicker frequency of the open fires is around 10 – 20Hz and declines relatively smoothly to the noise level. The fact that the radiation from a smoldering fire has characteristics similar to those of a hot surface poses special challenges to the detection of such fires especially in environments where hot surfaces are to be expected. However, since smoldering fires are likely to be away from kitchens and utility rooms, a fire detector could still be devised but caution will be needed in addressing the false alarm issues.

4. Conclusions

(1). The open test fires are very luminous and both gas band radiation and continuous soot radiation are evident. The radiation intensity from carbon dioxide and soot at 4.3 μm is more than two orders higher than that from soot, water, and carbon dioxide at 2.7 μm. For the two smoldering fires, TF2 and TF3, the continuous radiation from the smoldering surface is evident and the gas band radiation is hardly found, furthermore, the absorption in the carbon dioxide band in the room air at 4.3 μm is seen.

(2). The PDFs are clipped Gaussian in shape, especially for the carbon dioxide and soot band at 4.3 μm, where carbon dioxide radiation is dominant, is almost symmetric around the mean intensity value, however, in the case of open test fires, the PDF at 1.45 μm, where in-flame soot dominates the spectral radiation intensity, is not symmetric in shape, and shows a lognormal behavior. Because of the large fluctuations in soot radiation, the overall ranges are broad, which is not applied to the case of smoldering fires.

(3). The gas band CPDFs are steep because of the concentration fluctuations are strongly related to the level of mixing through the state relationships. On the other hand, the soot CPDF is flatter because various amounts of soot can exist at different levels of mixing depending on chemical kinetic and differential diffusion effects.

(4). Most of the energy of the fluctuations of the spectral radiation intensities in smoldering fires is below 2 or 3 Hz and declines very rapidly to the noise levels. However, flicker frequency of the open fires is around 10 – 20Hz and declines relatively smoothly to the noise level.

(5). TF3 was used as to study the mid infrared characteristics of smoldering fire, because, although it has same characteristics with TF2, the IR signature from TF2 is not so high, and as a result of this, there are some noises in PDFs, CPDFs, and PSDs of TF2.

5. Acknowledgement

This work was performed under the sponsorship of the U. S. Department of Commerce, National Institute of Standards and Technology under Grant No. 60NANB5D0113 with Dr. William Grosshandler and Dr. George Mullholand serving as the federal Program Officer.

References

[1] Grosshandler, W. L., An Assessment of Technologies for Advanced Fire Detection. Heat and Mass Transfer in Fire and Combustion Systems, HTD vol 223, ASME, New York, 1992:1-9.

[2] Middleton, J. F. Flame Detectors. Ninth International Conference on Automatic Fire Detection, AUBE 89, Duinsburg, Germany, 1989:143-154.

[3] Sivathanu, Y. R., and Tseng, L. K, Characterization of Radiation Properties of Fires Using Multi-Wavelength Measurements, Thirtieth section anniversary technical meeting, Central states section, The combustion institute, 1996:304-309.

[4] Lloyd, A. C., Development and Evaluation of Fire Detection Algorithm with Source Temperature Discrimination and Frequency Content, MSME Thesis, Purdue University, West Lafayette, IN, 1997.

[5] Sivathanu, Y. R. and Faeth, G. M., Temperature / Soot Volume Fraction Correlations in the Fuel-Rich Region of Buoyant Turbulent Diffusion Flames, Combustion and Flame, 1990;81:150-165.

[6] Sivathanu, Y. R., Gore, J. P., and Dolinar, J., Transient Scalar Properties of Strongly Radiating Jet Flames, Combustion Science and Technology, 1991;76:45-66.

[7] Sivathanu, Y. R., and Gore, J. P., Simultaneous Multiline Emission Absorption Measurements in Optically Thick Turbulent Flames, Combustion Science and Technology, 1991;80:1-21.

[8] CEN, Components of Automatic Fire Detection Systems: Fire Sensitivity Test, Part 9, European Committee for Standardization, Brussels, 1982.

[9] Ji, J., Gore, J. P., Sivathanu, Y. R., and Lim, J., Fast Infrared Array Spectrometer Used for Radiation Measurements of Lean Premixed Flames, 34th National Heat Transfer Conference, Pittsburgh, Pensylvania, 2000:1-6.